

A Hybrid Biped Stabilizer System Based on Analytical Control and Learning of Symmetrical Residual Physics

Mohammadreza Kasaei¹, Miguel Abreu², Nuno Lau¹, Artur Pereira¹ and Luís Paulo Reis²

¹IEETA/DETI, University of Aveiro 3810-193 Aveiro, Portugal

²LIACC/FEUP, Artificial Intelligence and Computer Science Lab, University of Porto, Portugal
{mohammadreza, nunolau, artur}@ua.pt, {m.abreu,lpreis}@fe.up.pt

Abstract—Although humanoid robots are made to resemble humans, their stability is not yet comparable to ours. When facing external disturbances, humans efficiently and unconsciously combine a set of strategies to regain stability. This work deals with the problem of developing a robust hybrid stabilizer system for biped robots. The Linear Inverted Pendulum (LIP) and Divergent Component of Motion (DCM) concepts are used to formulate the biped locomotion and stabilization as an analytical control framework. On top of that, a neural network with symmetric partial data augmentation learns residuals to adjust the joint's position, thus improving the robot's stability when facing external perturbations. The performance of the proposed framework was evaluated across a set of challenging simulation scenarios. The results show a considerable improvement over the baseline in recovering from large external forces. Moreover, the produced behaviors are human-like and robust to considerably noisy environments.

Keywords: Humanoid and bipedal locomotion, deep learning in robotics and automation, robust/adaptive control of robotic systems, learning residual physics

I. INTRODUCTION

Humanoid robots are extremely versatile and can be used in a wide range of applications. Nevertheless, robust locomotion is a challenging topic which still needs investigation. *Stability and safety* are essential requirements for a robot to act in a real environment. Humans combine a set of strategies (e.g. moving arms, ankles, hips, taking a step, etc.) to regain the stability after facing an external disturbance. The question is, *despite the humanoid robots' versatility, why are they not as capable as us?*

To find an answer to this question, we started by investigating the stabilizer systems of humanoid robots. The core of these systems is typically an abstract or accurate dynamics model of the robot, according to which, a set of controllers is designed to constantly cancel the effects of perturbations, such as external pushes, uneven terrains, and collisions with obstacles. Abstract models are used more often due to their simplicity and computational efficiency but also because they are platform independent and can be easily adapted to any type of humanoid robot.

The most widely used model in literature is the Linear Inverted Pendulum (LIP) which abstracts the overall dynamics of a robot as a single mass. It restricts the vertical movement of the mass to provide a linear model which yields a fast solution for real-time implementations.

This model has been investigated and extended for decades to design and analyze the balance controllers. Pratt et al. [1] introduced the Capture Point (CP) concept to improve the walking stability. Basically, the CP uses the current state of the COM to determine a 2D point on the floor where the robot should step to regain its stability. Later, Takanaka et al. [2] proposed the Divergent Component of Motion (DCM) concept that splits the LIP's dynamics into stable and unstable parts, such that controlling the unstable part is enough for keeping the stability. In [3] DCM has been extended to 3D and, based on that, the Enhanced Centroidal Moment Pivot point (eCMP) and also the Virtual Repellent Point (VRP) have been introduced, which could be used to encode the direction, magnitude and total forces of the external push. Using these concepts, several control approaches including classical feedback controllers [4]–[6], Linear Quadratic Regulator (LQR)-based methods [7]–[10] and the Model Predictive Control (MPC) [11]–[13] have been proposed to formulate the stabilizer system. All of them are trying to compensate the tracking error by using a combination of three strategies which are: manipulating the Ground Reaction Force (GRF) and modifying the position and the time of the next step. Recently, researchers are investigating about releasing the assumptions of LIP (e.g. vertical motion of the COM and its angular momentum) which causes dealing with nonlinearities [14]–[16]. The stability of humanoid robots has significantly improved but they are not stable and safe enough to be utilized in our daily-life environments.

To answer the question raised in the beginning, we looked at how humans learn recovery strategies. We rely on past experiences to improve our methods. After a few years, we have a solid locomotion strategy, on top of which is easy to learn new things. Therefore, learning recovery strategies is just a matter of efficiently combining our locomotion gait with additional residual reactions. In this paper, we propose a stabilizer system for humanoid robots which is based on a tight coupling between analytical control and machine learning. An overview of this system is depicted in Fig. 1. Specifically, we use LIP to analytically formulate biped locomotion and recovery strategies, and combine it with a symmetry-enhanced optimization framework based on the Proximal Policy Optimization (PPO) [17] to learn residual physics — a concept coined by Zeng et al. [18]. The learned policy adjusts a set of parameters of the analytical

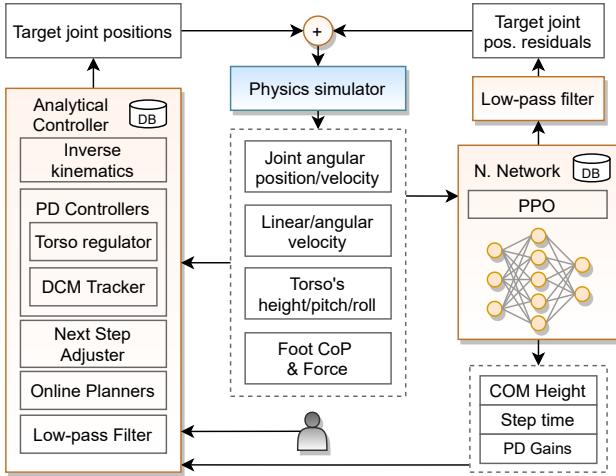


Fig. 1. An overview of the proposed stabilizer system. The highlighted boxes represent the main modules and the white boxes are the exchanged information among them.

controller and learns a set of model-free skills to regain stability.

Our approach is applied to the COMAN robot [19], which, like most humanoid models, has reflection symmetry in the sagittal plane. Human-like behaviors are hard to characterize. However, we highlight some aspects which are commonly associated with human gaits, such as motion fluidity, pattern repetition and symmetry. The former aspect is dependent on the mechanical part of the robot, since a low-level controller can easily produce fluid movements. The repetition of a pattern can be guided by an analytical controller, working as a foundation to learn more complex skills. Finally, the notion of symmetry can be analyzed through two points of view. On the one hand, humans show a clear bias towards symmetry, often associating positive reactions with symmetry and negative reactions with asymmetry [20]. From this perspective, perfect symmetry follows the concept of classical beauty immortalized by Leonardo da Vinci's Vitruvian Man. On the other hand, real humans are not perfectly symmetrical, and, according to Handžić and Reed, unbalanced gait patterns can be perceived as unimpaired or normal, within reason [21]. Therefore, in the context of human-like behaviors, the symmetry of a model should be leveraged when developing biped locomotion, but not to the point where it becomes a hard constraint.

Leveraging model symmetries using domain knowledge is a widely used technique in machine learning approaches. Data augmentation is a straightforward method to achieve that goal, being popular in supervised learning at least since Baird et al. in 1992 [22], according to Chen et al. [23], and gaining momentum in reinforcement learning [24]–[28]. We propose a learning framework where the data is only partially augmented, leveraging the symmetry to improve learning time and human-likeness without restricting asymmetric movements too much, thus widening the range of possible behaviors.

II. RELATED WORK

Several approaches for stabilizing a humanoid have been proposed that can be categorized into three major categories. In the remainder of this section, these categories will be introduced and some recent works in each category will be briefly reviewed.

A. Analytical Approaches

The basic idea behind the approaches in this category is using an abstract or accurate dynamics model of the robot and designing a set of controllers based on some criteria to minimize the tracking error.

Griffin et al. [29] proposed a walking stabilizer system based on adjusting the step time and position. They proposed a simple step time adjustment algorithm to speed up the swing leg for setting the foot down quickly to recover from an error. Additionally, they developed a quadratic program to combine the abilities of a center of pressure (COP) feedback controller and a step adjustment algorithm. This combination provides an optimized reference trajectory based on foot step adjustments which takes into account the COP feedback control. The performance of their approaches has been validated using simulations and real robot experiments.

Jeong et al. [30] developed a walking controller based on online optimization of three push recovery strategies: ankle, hip, and stepping strategies. They used Linear Inverted Pendulum Plus Flywheel (LIPFM) as their dynamics model. This model is an enhanced version of LIP that considers the momentum around the COM. They combined all the strategies, including the step time adjustment, based on a set of weighting factors, using an optimization program. The performance of their approach was shown by a set of simulations, including abstract and accurate model dynamics. They argued that their approach is practical enough to be deployed on real hardware and validated that with real robot experiments.

Stephane Caron [14] used a variable-height inverted pendulum (VHIP) to design a biped stabilizer based on linear feedback. They argued that VHIP is simple to implement and also more tractable in comparison with the 3D version of DCM because of its linear dynamics. Using this abstract model, they introduced a new push recovery strategy which utilizes the vertical motion of the COM to recover from severe perturbations. They set up an experiment using a real HRP-4 humanoid robot to show the performance of their method. They showed that the behavior of their stabilizer is similar to LIP once the Zero Momentum Point (ZMP) is inside the support polygon, and the height variations were enabled when the ZMP reached the support polygon's edges.

Khadiv et al. [31] argued that adjusting the time and position of the next step is sufficient to improve the locomotion robustness. They proposed a simple and optimal walking pattern generator that was able to select the next step location and timing at every control cycle. The performance of their approach has been validated using a simulated humanoid robot with passive ankles through different simulation scenarios, including push recovery and foot slippage.

B. Machine Learning Approaches

The approaches in this category are designed to learn a feasible policy through interaction with the environment. Nowadays, Deep Reinforcement Learning (DRL) has shown its capability by solving complex locomotion and manipulation tasks, which are generally composed of high-dimensional continuous observation and action spaces [32], [33].

Data augmentation in reinforcement learning is widely used to improve the optimization performance but, in this work, we restrict the scope to symmetry oriented solutions. In the context of supervised learning, it is worth mentioning that RL can also be used as a means to generate data augmentation policies [34]. Agostini et al. [24] differentiate between spatial and temporal symmetry, where the former considers spacial transformations such as reflection and rotation, and the latter considers time transformations, such as time inversion. Since our model is not a conservative system, the latter is not applicable, as time inversion symmetry requires no energy loss (e.g. due to friction). One of the proposed solutions to exploit spatial symmetries on an inverted pendulum is to generate symmetric data from actual samples, and feed that information to the optimization algorithm. In literature, this process is used to control distinct models performing numerous tasks, which include teaching a real dual-armed humanoid robot how to move objects [26], incorporate symmetry in the walking gait of various humanoid models [25] and a quadruped [27] (which has more than one plane of symmetry), and even reducing the complexity of GO through a dihedral group of 8 reflections and rotations [28].

C. Hybrid Approaches

The approaches in this category are focused on combining the potential of both aforementioned categories. To do so, learning algorithms are used on top of physics-based controllers to predict the controllers parameters and to learn residual physics, which can lead to impressively accurate behaviors [18], [35].

Yang et al. [35] designed a hierarchical framework based on DRL to ensure the stability of a humanoid robot by learning motor skills. Their framework is composed of two independent layers, the high-level layer generates a set of joint angles and the low-level layer translates those angles to joint torques using a set of PD controllers. In their approach, the reward function was composed of six distinct terms that were mostly related to the traditional push recovery strategies, and it was obtained by adding all terms together with different weights. They showed the performance of their approach using a set of simulations with a simulated NASA Valkyrie robot. The results demonstrated that the robot learned how to regain its stability while facing external disturbances.

Tsounis et al. [36] combined model-based motion planning and DRL to realize terrain-aware locomotion for quadruped robots. They decomposed locomotion into main parts and independently trained them using model-free DRL to plan and execute foothold and base motions. They demonstrated

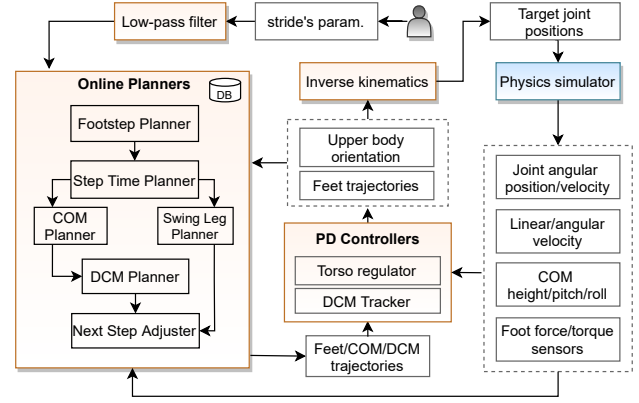


Fig. 2. Overview of the proposed analytical controller. The online planners module generates a set of reference trajectories according to the input command and the states of the system constantly. The PD controllers module is responsible for tracking the generated trajectories. The highlighted boxes represent the main modules and the white boxes are the exchanged information among them.

the performance of the approach using a suite of challenging terrains, including uneven terrain, gaps and stepping-stones. The simulation results showed that the simulated robot overcame all the challenges successfully.

According to the aforementioned works, we believe that using machine learning on top of analytical approaches is the key to open doors for humanoid robots to step out of laboratories. In the remainder of this paper, we will describe the design of a framework composed of an analytical controller and a DRL algorithm, used to learn residual physics.

III. ANALYTICAL CONTROLLER

In this section, the structure of our analytical controller will be presented. The overall architecture of this controller is depicted in Fig. 2. The core of this controller is based on the LIP and DCM concepts. The proposed controller is composed of two main modules: Online Planners and PD Controllers. Online Planners is responsible for generating the reference trajectories according to the stride's parameters provided by the user, the robot's state and the controllers' output. PD Controllers is responsible for regulating the upper body orientation and tracking the planned trajectories to generate closed-loop locomotion. The corresponding target joint positions will be generated using the Inverse Kinematics, which takes into account kinematic feasibility constraints. The target joint positions will be fed into the Physics Simulator, which is responsible for simulating the interaction of the robot with the environment and producing sensory information, as well as the global position and orientation of the robot in the simulated environment. In the rest of this section, the details of PD Controllers and Online Planners will be explained.

A. Regulating the Upper Body Orientation

The upper body of a humanoid is generally composed of several joints. While the robot is walking, their motions and vibrations generate angular momentum around the COM. LIP-based models do not take this momentum into account

and consider that the GRF always passes through the COM. To cancel the effects of this momentum, we designed a PD controller based on the inertial sensor values that are mounted on the robot's torso:

$$\dot{\Phi} - \dot{\Phi}_d = -K_\Phi(\Phi - \Phi_d) \quad , \quad (1)$$

where $\Phi = [\Phi_{roll} \ \Phi_{pitch}]^\top$ is the angle of the torso, $\dot{\Phi}$ represents the angular velocity of the torso, Φ_d denotes the desired state of the torso and K_Φ is the controller gain.

B. DCM Tracker

According to LIP model, the dynamics model of a humanoid robot can be represented using the following differential equation:

$$\ddot{c} = \omega^2(c - p) \quad , \quad (2)$$

where $c = [c_x \ c_y]^\top$ is the position of the COM, $p = [p_x \ p_y]^\top$ represents the position of the ZMP, $\omega = \sqrt{\frac{g}{c_z}}$ is the natural frequency of the pendulum, where g is the gravity constant and c_z represents the height of the COM. The DCM for this model is defined as:

$$\zeta = c + \frac{\dot{c}}{\omega} \quad , \quad (3)$$

where $\zeta = [\zeta_x \ \zeta_y]^\top$ is the DCM and \dot{c} is the velocity of the COM. By taking the time derivative of this equation and substituting (2) into the result, LIP dynamics can be represented by a linear state space system as follows:

$$\frac{d}{dt} \begin{bmatrix} c \\ \zeta \end{bmatrix} = \begin{bmatrix} -\omega & \omega \\ 0 & \omega \end{bmatrix} \begin{bmatrix} c \\ \zeta \end{bmatrix} + \begin{bmatrix} 0 \\ -\omega \end{bmatrix} p \quad . \quad (4)$$

This system shows that the COM is always converging to the DCM, and controlling the DCM is enough to develop a stable locomotion. Consequently, the DCM tracker can be formulated as follows:

$$\dot{\zeta} - \dot{\zeta}_d = -K_\zeta(\zeta - \zeta_d) \quad , \quad (5)$$

where K_ζ represents the controller gains, $\zeta_d, \dot{\zeta}_d$ are the desired DCM and its time derivative, which are generated by the DCM planner (see Fig. 2). It should be mentioned that the controllers' gains have been tuned by an expert.

C. Online Planners

As shown in Fig 2, Online Planners is composed of a set of sub-planners which are solved separately and connected together hierarchically to reduce the complexity of the planning process. The planning process is started by generating a set of footsteps ($f_i = [f_{ix} \ f_{iy}]^\top \ i \in \mathbb{N}$) according to the input stride's parameters and the current feet configuration. Then, the step time planner assigns a set of timestamps to the generated footstep according to the stride duration. Afterwards, to have a smooth trajectory during lifting and landing of the swing foot, a cubic spline is used to generate the swing leg trajectory based on the generated footsteps and a predefined swing height. Accordingly, the COM planner generates the COM trajectory by solving (2) as a boundary value problem based on the generated footsteps:

$$c = f_i + \frac{(f_i - c_f) \sinh(\omega(t - t_0)) + (c_0 - f_i) \sinh(\omega(t - t_f))}{\sinh(\omega(t_0 - t_f))} \quad , \quad (6)$$

where t_0, t_f, c_0, c_f are the times and corresponding positions of the COM at the beginning and end of a step, respectively. c_f is assumed to be between the current support foot and the next support foot ($\frac{f_i + f_{i+1}}{2}$). After generating the COM trajectory, the DCM trajectory can be obtained by substituting (6) and its time derivative into (3). This trajectory will be fed into PD Controllers to generate closed-loop locomotion.

In some situations, such as when the robot is being pushed severely, the DCM tracker cannot track the reference because of the controllers' output saturation. In such conditions, humans adjust the next step time and location, in addition to the COM's height. Equation (3) is an ordinary differential equation. Due to the observability of DCM at each control cycle, the position of the next step can be determined by solving this equation as an initial value problem:

$$f_{i+1} = f_i + (\zeta_t - f_i) e^{\omega(T-t)} \quad , \quad (7)$$

where f_i, f_{i+1} are the current and next support foot positions and t, T denote the time and stride duration, respectively. It should be noted that adjusting the next step time as well as the height of the COM are challenging because of the nonlinearities. In the next section, we explain how these parameters can be adjusted through a machine learning approach.

IV. LEARNING RESIDUAL PHYSICS

Although the presented analytical controller framework is able to keep the stability of the robot and generate stable locomotion, it does not generalize well to unforeseen circumstances. In this section, we introduce a learning framework designed to learn residual physics on top of the analytical controller. The objective is to regulate control parameters such as the COM height and step length, but also learn model-free skills by adjusting some of the robot's joint positions.

A. Formal structure

The learning framework extends the PPO algorithm with symmetric data augmentation based on static domain knowledge. Like most humanoid models, the COMAN robot has reflection symmetry in the sagittal plane. This knowledge can be leveraged to reduce the learning time and guide the optimization algorithm in creating a human-like behavior.

This learning problem can be formally described as a Markov Decision Process (MDP) – a tuple $\langle S, A, \Psi, p, r \rangle$, where S is the set of states, A is the set of actions, $\Psi \subseteq S \times A$ is the set of admissible state-action pairs, $p(s, a, s') : \Psi \times S \rightarrow [0, 1]$ is the transition function, and $r(s, a) : \Psi \rightarrow \mathbb{R}$ is the reward function. In order to reduce the mathematical model by exploiting its redundancy and symmetry, Ravindran and Barto [37] proposed the MDP homomorphism formalism, which describes a transformation

that simplifies equivalent states and actions. Let h be an MDP homomorphism from $M = \langle S, A, \Psi, p, r \rangle$ to $M' = \langle S', A', \Psi', p', r' \rangle$, and A_s be the set of admissible actions in state s . The concept of MDP symmetries is a special case of this framework where $f : S \rightarrow S'$ and $g_s : A_s \rightarrow A'_{f(s)}$ are bijective functions. An MDP isomorphism from and to the same MDP can be considered an automorphism that satisfies:

$$p(f(s), g_s(a), f(s')) = p(s, a, s'), \quad \forall s, s' \in S, a \in A_s, \quad (8)$$

$$\text{and } r(f(s), g_s(a)) = r(s, a), \quad \forall s \in S, a \in A_s. \quad (9)$$

B. Data augmentation

In this work, the formulated problem is optimized using PPO [17], an actor-critic algorithm that uses a clipping function to constrain the policy update directly inside the objective function, thus preventing it from being too greedy. After performing a grid search, the batch size was set to 8192 samples and the learning rate to $3e-4$ (using a linear scheduler). For each episode, an MDP trajectory j is characterized by a sequence of states, actions and rewards such that $j = \{S_0, A_0, R_0, S_1, A_1, R_1, \dots\}$. Each trajectory is used to produce a set of samples $k = \{\{S_0, A_0, Ad_0, V_0\}, \{S_1, A_1, Ad_1, V_1\}, \dots\}$, where V_i is obtained from the λ -return as defined by Sutton and Barto [38], and serves as value target for the update function; and Ad_i is the generalized advantage estimate [39]. Our proposal is to partially augment data by copying and transforming only a fraction of the acquired samples. Different augmentation ratios are tested in Section VI. As an example, consider the addition of symmetrical samples with a ratio of 50%. Following the condition established in (9), each batch of samples is artificially built as $\{W_1, W_2, u(W_2), W_3, W_4, u(W_4), \dots\}$ where $u(W_i) = \{f(S_i), g_s(A_i), Ad_i, V_i\}$. The observations' normalization is continuously updated by calculating the mean and standard deviation of each observation. However, both of these metrics are shared among the two symmetric groups to ensure that no asymmetrical bias is introduced.

C. Network Architecture

The network architecture as well as the system space and action space parameters are represented in Fig. 3. The observations comprise the position of 6 joints: shoulder, hip and waist with 3 degrees of freedom (DoF), ankle with 2 DoF, knee and elbow with 1 DoF. Considering that all joints are mirrored except the waist, there are 23 joint variables. Additional observations include the foot center of pressure (relative to its center, in x and y) and respective force magnitude, the torso's linear and angular velocity, height, pitch, and roll; totalling 38 state space variables. This information is fed to a neural network composed of two hidden layers of 64 neurons, producing 27 continuous values that control some joints' actuators, two high-level parameters (the step length and COM height) and two PD gain vectors (K_Φ from (1) and K_C from (5)). The high-level parameters regulate the analytical controller by providing the duration

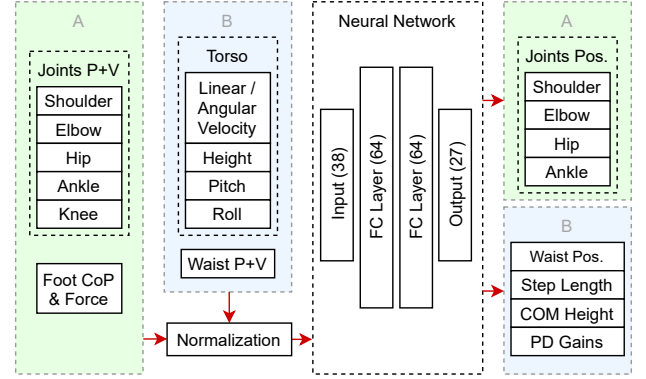


Fig. 3. Network architecture, system space parameters and symmetry transformation groups used for data augmentation: reflection symmetry transformation (A) and no transformation or inversion (B).

of each step and the COM height, needed to generate the leg joint trajectories. The joint positions are controlled with residuals, which are added to the precomputed trajectories.

Both the state space and action space parameters are grouped in two categories, according to the symmetry transformations used for data augmentation. Category A includes duplicated observations that are mirrored, considering the reflection symmetry in the sagittal plane. Category B includes unique observations that may remain unchanged or suffer an inversion transformation. As an example, the torso's height and pitch are not transformed when generating symmetric samples, but the roll angle is inverted. The linear and angular velocities are common in some axes, and inverted in others to obtain their symmetric counterparts.

D. Reward function

The reward function tries to convey one fundamental goal — balance — while motivating cyclic movement patterns. The balance goal seeks to keep the robot on its feet in all situations. The subgoal of performing cyclic movement patterns has the purpose of improving the human-like aspect of the behavior, according to the characterization given in Section I. Specifically, it tries to reduce the neural network's influence (NNI) when there is no need to intervene. Both of these notions can be expressed through the following reward:

$$R = 1 - \frac{1}{J} \sum_i^J \frac{|\delta_i|}{S_i}, \quad (10)$$

where δ_i is the residual applied to the position of joint i , J is the number of joints, and S_i is the residual saturation value. It is important to note that the NNI component's objective is not to reduce the energy consumption or range of motion, since it is only applied to the residuals and not the hybrid controller's output.

V. SIMULATION SCENARIOS

To validate the performance of the proposed framework, a set of two learning scenarios and one test scenario has been

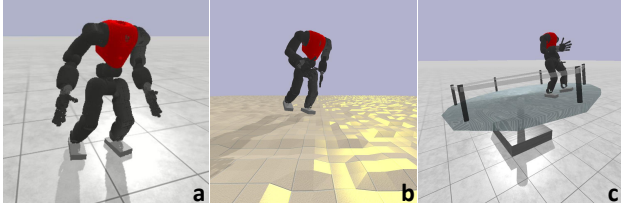


Fig. 4. Simulation scenarios. The robot learns how to recover from external forces in a flat surface (a) and in an uneven terrain with perturbations that can reach 2cm (b). It then faces unseen circumstances when it is placed on a tilting platform that moves erratically (c).

designed. The goal of this structure is to prepare the physical robot to handle real world adverse conditions. We use the COMAN robot in PyBullet [40] – an environment based on the open source Bullet Physics Engine. The simulated robot is 95cm tall, weighs 31kg, and has 23 joints (6 per leg, 4 per arm and 3 between the hip and the torso).

A. Scenario L1

The first learning scenario is composed of a flat platform (see Fig. 4a), where the robot is initially placed in a neutral pose. It then starts to walk in place, while being pushed by an external force at random intervals, between 2.5 and 3.0 seconds. The force is applied for 25ms and ranges from 500N to 850N. Its point of application is fixed at the torso’s center and its direction is determined randomly in a 2D plane parallel to the ground. The robot’s objective is to avoid falling. The episode ends when the robot’s height drops below 0.35m or any of its body parts (except the feet) touches the ground.

B. Scenario L2

The second learning scenario is an extension of the first one, where the flat surface is replaced by an uneven terrain with perturbations that can reach 0.02m, as depicted in Fig. 4b. The external force dynamics are the same as in scenario L1.

C. Scenario T1

The test scenario was designed to evaluate the generalization capabilities of the hybrid controller in unexpected circumstances. It is characterized by a tilting cylindrical platform (see Fig. 4c), which is supported by two actuators that move on the x and y axes, and range between -15 deg and 15 deg. The position of each actuator is given by adding a random component $r \in [-8^\circ, 8^\circ]$ to a correcting component $c = 0.35 \times P$, where P is the position of the robot in the opposite axis to the actuator. The goal of the latter component is to keep the robot on top of the platform by encouraging it to move to the center. The episode starts in a neutral state with the robot walking in place, and it ends when the robot falls, as in the previous scenarios.

VI. EXPERIMENTS

Five different symmetry ratios were tested per learning scenario, totalling ten different configurations. The symmetry

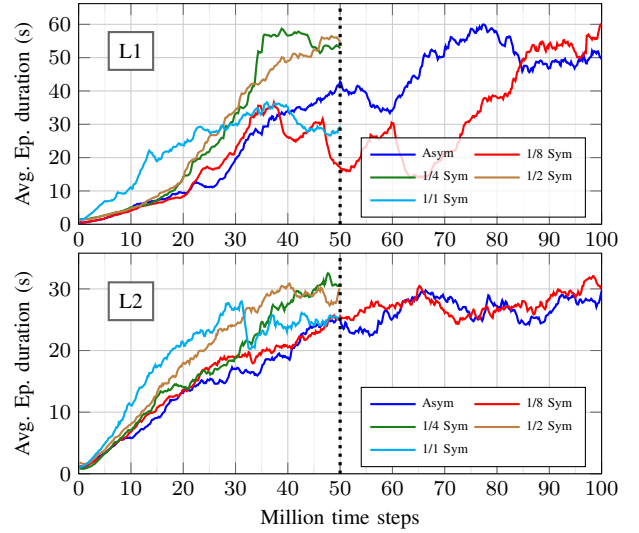


Fig. 5. Learning curves for the best models trained in scenario L1 (above) and L2 (below), under different symmetry configurations.

ratios were 0 (no data augmentation), 1/8 (1 symmetrical sample is generated per 8 acquired samples), 1/4, 1/2 and 1/1 (full symmetry). For each configuration, five models were trained. Fig. 4 depicts the learning curves for the best model in each configuration. The results are grouped according to the training scenario (L1 above and L2 below). Most optimizations ran for 50M time steps. However, the asymmetric and 1/8 symmetry configurations needed 100M time steps to reach a plateau. For the configurations that included data augmentation, the best performing ratios were 1/4 and 1/2, with very similar results. In a subjective visual evaluation, the 1/2 ratio model seems to be marginally better in producing a human-like behavior. For the remainder of this section, we will compare in greater detail the asymmetric version with the 1/2 symmetric version. Videos of the results are available at <https://youtu.be/Lk9Wjha7RHw>.

It is important to note that the average episode duration reported by these learning curves results from a stochastic policy with a non-negligible random component. To better assess the optimized models, they were tested in each scenario (including T1 — the only test scenario) for 1000 episodes using the corresponding deterministic policy. Moreover, considering the 50M time steps target, and to be fair with every approach, only the evolution until 50M time steps was considered in these tests. Table I compares the average performance of four models against the baseline. The first four columns indicate, in this order, the episode duration, in seconds, in scenario L1, L2 and T1; and the neural network influence. The last column will be analyzed later in this section.

The baseline version (without residuals) is not able to handle the strong external forces applied in scenario L1, falling on average after 3.47s, which is typically after the first push is applied. On L2, it falls almost immediately due to the floor perturbations, an outcome which is also seen in T1. All four learned models are a great improvement over

TABLE I
AVERAGE RESULTS PER LEARNING CONFIGURATION

Learning configuration	Episode duration (s)			N. Network Influence	M. Sym. Index
	L1	L2	T1		
Baseline	3.47	1.51	1.87	-	-
L1 Asym	104.5	5.1	4.8	0.072	1.42
L1 1/2 Sym	202.2	4.6	4.8	0.055	1.19
L2 Asym	321.9	34.2	27.8	0.165	1.23
L2 1/2 Sym	193.7	43.5	21.0	0.127	0.99

the baseline. As expected, the last two models that learned on L2 were able to generalize successfully when tested on L1 or T1, and, on the opposite side, the models that learned on L1 did not perform well in unforeseen circumstances.

However, some results were not expected. During training, the symmetrically-enhanced models performed better than their counterparts, but while testing in distinct scenarios, the asymmetrical models generalized better. Another interesting result is that the asymmetrical L1 model performed worse in its own scenario (104.5s) than the asymmetrical L2 model (321.9s).

To better understand this outcome, we need to analyze the neural network influence column, whose metric is explained in (10). Since L2 and L2 Sym are the most challenging scenarios, the robot learned to sacrifice its immediate reward by applying larger residuals in order to survive for a longer period. Naturally, this is a trade-off between cyclic movement patterns and raw performance. Moreover, learning an asymmetrical behavior can arguably be considered more challenging, which, in this case, has led to a higher network influence. So, in essence, that may explain why it generalizes better than its symmetrical counterpart.

A. Symmetry analysis

The analytical controller produces symmetrical trajectories upon which the neural network residuals are applied. To evaluate the residuals symmetry, we built upon the concept of Symmetry Index (SI) proposed by Robinson et. al [41]. The original method compares the kinematic properties of each lower limb. To address the issues caused by abstracting the kinematic properties of each joint, we propose the Mirrored Symmetry Index (MSI):

$$MSI = \frac{\|\delta_t - \delta'_t\|_1}{0.5 \times (\|\delta_t\|_1 + \|\delta'_t\|_1)}, \quad (11)$$

where $\delta_t = [\delta_1^t, \dots, \delta_n^t]$ is the vector of residuals applied to each joint during time t , $\|\cdot\|_1$ is the ℓ_1 -norm, and δ'_t is the vector of residuals applied to the symmetric set of joints if the current state was also symmetrically transformed, i.e., $\delta'_t \sim \pi(\cdot|f(S_t))$, where π is a stochastic policy. Instead of evaluating an average kinematic feature, the MSI computes a symmetry index at each instant, which can then be averaged for a full trajectory to obtain a global symmetry assessment.

As seen in Table I, the models which were learned using the data augmentation method obtained a lower MSI value, when compared to the other two models. The results do not show a large reduction, which can be explained by

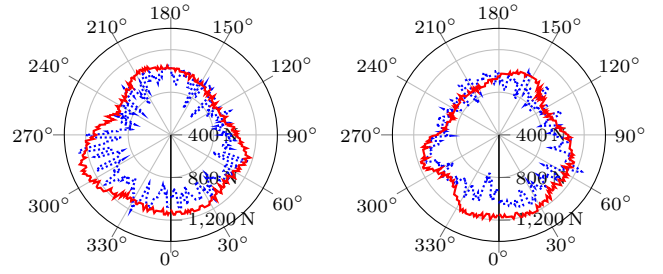


Fig. 6. Maximum radially applied external force from which the robot can consistently recover as a function of the direction of application, where zero degrees corresponds to the front of the robot. On the left is shown the model which learned on L2 Sym and on the right L2. The force was applied both in the flat terrain (solid red line) and the uneven terrain (dotted blue line).

the analytical controller's role in regulating the trajectory symmetry, and the relaxed data augmentation restriction imposed to the network.

To assess the notion of symmetry on a practical scenario, the models trained on L2 and L2 Sym were submitted to a test where an external force with constantly increasing norm is radially applied to the robot in a given direction. When the robot is no longer able to recover consistently (more than 50% of the trials), the maximum force is registered and another direction is tested. The result can be seen in Fig. 6 on the flat terrain (solid red line) and uneven terrain (dotted blue line). In both cases, the robot is able to better withstand forces that are applied to the front (around 0 deg). On one side, the symmetrically-enhanced version presents a more balanced result, which can be visually perceived. On the other side, the asymmetrical model can withstand larger forces in a specific range around 300 deg. This difference consists of a trade-off between symmetry and raw performance.

B. Drift

Another way of objectively assessing the influence of symmetry in the learned behaviors is to compare the resulting models in terms of position drift, while walking in place. This experiment was performed for 500 seconds, in scenario L1, without any external force being applied to the robot. Initially, the robot is placed at (0,0) and it is instructed to walk in place. Fig. 7 shows the path described by the baseline (green), solely composed by the analytical controller; the L1 1/2 Sym model (red); and the L1 Asym model (blue). A video demonstration is available at <https://youtu.be/Lk9Wjha7RHw>. All models perform some form of drift over time. However, due to its asymmetry bias, the L1 Asym model had the worst results. Sampling the position at every 5 seconds, the total travelled distance was 18.09m for the L1 Asym model, 2.60m for the L1 1/2 model, and 3.51m for the baseline. Although a high-level controller could compensate for the model bias and eliminate the drift, lowering the need for regulation is always desirable.

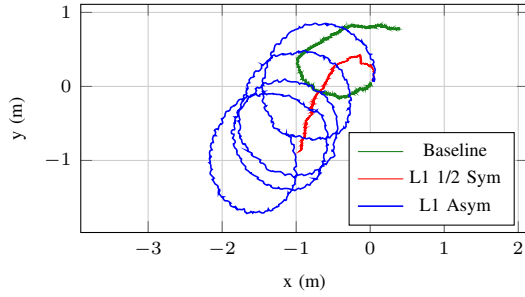


Fig. 7. Drift comparison, while walking in place for 500s, for the baseline (red), the L1 Asym model (orange) and the L1 1/2 Sym model (yellow).

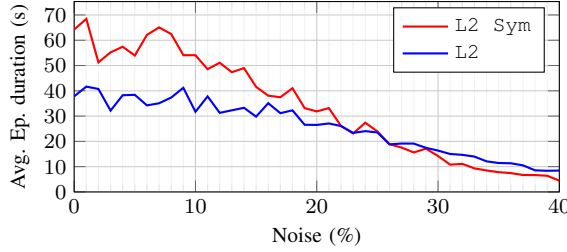


Fig. 8. Average episode duration as a function of noise applied to the state observations for the symmetrical (red line) and asymmetrical (blue line) models learned and tested on the uneven terrain.

C. Noise robustness

Finally, we present a noise robustness analysis, which is a matter of significant concern on real applications. To test this, the state variables are multiplied by a random factor that follows a uniform distribution $z \sim \mathcal{U}(1.0, N)$ where N ranges from 1.0 to 1.4, i.e., 0% to 40% of maximum noise. Fig. 8 shows the average impact of this artificial perturbation on the average episode duration, on the uneven terrain scenario, while being pushed by an external force with the same dynamics as described in Section V-A, with a fixed interval of 3.5 seconds. Both the symmetrical and asymmetrical models can withstand a maximum noise of 20% without dropping below the 30s mark, which attests the models robustness in considerably noisy scenarios.

VII. CONCLUSION

In this paper, we tackled the problem of developing a robust stabilizer system for humanoid robots. We proposed a framework based on a tight coupling between analytical control and deep reinforcement learning to combine the potential of both approaches. First, we used the LIP and DCM concepts to develop an analytical control framework to generate robust locomotion. Then, we designed a learning framework which extends the PPO algorithm with symmetric partial data augmentation to learn residuals on top of the analytical approach. This hybrid approach aims at unlocking the full potential of the robot by exploiting the consistency of the analytical solution, the adaptability of neural networks to adjust the control parameters in unforeseen circumstances, and the model's symmetry, while not totally constraining the exploration of asymmetric reactions.

The results attest the models' robustness in considerably noisy environments. The symmetry enhanced models were able to perform better in the scenarios where they learned, but were not able to generalize as well in unforeseen circumstances. However, the difference is partially explained by the way the reward function's influence penalty is less restrictive in challenging conditions. In comparison with an asymmetric approach, our symmetry learning method was more sample efficient and produced a behavior with less position drift, lowering the need for regulation in a high-level controller. In the future, we would like to explore the application of this hybrid approach on other types of gait, including running and climbing. Preliminary results show that the models trained in this work already generalize well to other gaits, such as walking forward, but are not yet ready for changes of direction or side walking.

REFERENCES

- [1] J. Pratt, J. Carff, S. Drakunov, and A. Goswami, "Capture point: A step toward humanoid push recovery," in *2006 6th IEEE-RAS International conference on humanoid robots*. IEEE, 2006, pp. 200–207.
- [2] T. Takenaka, T. Matsumoto, and T. Yoshiike, "Real time motion generation and control for biped robot-1st report: Walking gait pattern generation," in *Intelligent Robots and Systems, 2009. IROS 2009. IEEE/RSJ International Conference on*. IEEE, 2009, pp. 1084–1091.
- [3] J. Engelsberger, C. Ott, and A. Albu-Schäffer, "Three-dimensional bipedal walking control based on divergent component of motion," *IEEE Transactions on Robotics*, vol. 31, no. 2, pp. 355–368, 2015.
- [4] T. Komura, H. Leung, S. Kudoh, and J. Kuffner, "A feedback controller for biped humanoids that can counteract large perturbations during gait," in *Proceedings of the 2005 IEEE International Conference on Robotics and Automation*. IEEE, 2005, pp. 1989–1995.
- [5] J. Engelsberger and C. Ott, "Integration of vertical com motion and angular momentum in an extended capture point tracking controller for bipedal walking," in *2012 12th IEEE-RAS International Conference on Humanoid Robots (Humanoids 2012)*. IEEE, 2012, pp. 183–189.
- [6] M. Morisawa, N. Kita, S. Nakaoka, K. Kaneko, S. Kajita, and F. Kanehiro, "Biped locomotion control for uneven terrain with narrow support region," in *System Integration (SII), 2014 IEEE/SICE International Symposium on*. IEEE, 2014, pp. 34–39.
- [7] S. Kuindersma, F. Permenter, and R. Tedrake, "An efficiently solvable quadratic program for stabilizing dynamic locomotion," in *2014 IEEE International Conference on Robotics and Automation (ICRA)*. IEEE, 2014, pp. 2589–2594.
- [8] S. Mason, N. Rotella, S. Schaal, and L. Righetti, "Balancing and walking using full dynamics lqr control with contact constraints," in *2016 IEEE-RAS 16th International Conference on Humanoid Robots (Humanoids)*. IEEE, 2016, pp. 63–68.
- [9] S. Faraji, H. Razavi, and A. J. Ijspeert, "Bipedal walking and push recovery with a stepping strategy based on time-projection control," *The International Journal of Robotics Research*, vol. 38, no. 5, pp. 587–611, 2019.
- [10] M. Kasaei, N. Lau, and A. Pereira, "A robust biped locomotion based on linear-quadratic-gaussian controller and divergent component of motion," in *2019 IEEE/RSJ International Conference on Intelligent Robots and Systems (IROS)*, 2019, pp. 1429–1434.
- [11] P.-B. Wieber, "Trajectory free linear model predictive control for stable walking in the presence of strong perturbations," in *2006 6th IEEE-RAS International Conference on Humanoid Robots*. IEEE, 2006, pp. 137–142.
- [12] A. Herdt, N. Perrin, and P.-B. Wieber, "Walking without thinking about it," in *Intelligent Robots and Systems (IROS), 2010 IEEE/RSJ International Conference on*. IEEE, 2010, pp. 190–195.
- [13] C. Brasseur, A. Sherikov, C. Collette, D. Dimitrov, and P.-B. Wieber, "A robust linear mpc approach to online generation of 3d biped walking motion," in *2015 IEEE-RAS 15th International Conference on Humanoid Robots (Humanoids)*. IEEE, 2015, pp. 595–601.

- [14] S. Caron, "Biped stabilization by linear feedback of the variable-height inverted pendulum model," in *IEEE International Conference on Robotics and Automation*, May 2020. [Online]. Available: <https://hal.archives-ouvertes.fr/hal-02289919>
- [15] S. Kajita, M. Benallegue, R. Cisneros, T. Sakaguchi, S. Nakaoka, M. Morisawa, H. Kaminaga, I. Kumagai, K. Kaneko, and F. Kanehiro, "Biped gait control based on spatially quantized dynamics," in *2018 IEEE-RAS 18th International Conference on Humanoid Robots (Humanoids)*. IEEE, 2018, pp. 75–81.
- [16] T. Seyde, A. Shrivastava, J. Engelsberger, S. Bertrand, J. Pratt, and R. J. Griffin, "Inclusion of angular momentum during planning for capture point based walking," in *2018 IEEE International Conference on Robotics and Automation (ICRA)*. IEEE, 2018, pp. 1791–1798.
- [17] J. Schulman, F. Wolski, P. Dhariwal, A. Radford, and O. Klimov, "Proximal policy optimization algorithms," arXiv preprint arXiv:1707.06347, 2017.
- [18] A. Zeng, S. Song, J. Lee, A. Rodriguez, and T. Funkhouser, "Tossing-bot: Learning to throw arbitrary objects with residual physics," *IEEE Transactions on Robotics*, 2020.
- [19] E. Spyarakos-Papastavridis, G. A. Medrano-Cerda, N. G. Tsarakis, J. S. Dai, and D. G. Caldwell, "A push recovery strategy for a passively compliant humanoid robot using decentralized lqr controllers," in *2013 IEEE International Conference on Mechatronics (ICM)*. IEEE, 2013, pp. 464–470.
- [20] D. W. Evans, P. T. Orr, S. M. Lazar, D. Breton, J. Gerard, D. H. Ledbetter, K. Janosco, J. Dotts, and H. Batchelder, "Human preferences for symmetry: Subjective experience, cognitive conflict and cortical brain activity," *PLoS ONE*, vol. 7, no. 6, 2012.
- [21] I. Handžić and K. B. Reed, "Perception of gait patterns that deviate from normal and symmetric biped locomotion," *Frontiers in psychology*, vol. 6, p. 199, 2015.
- [22] H. S. Baird, H. Bunke, and K. Yamamoto, *Structured document image analysis*. Springer Science & Business Media, 2012.
- [23] S. Chen, E. Dobriban, and J. H. Lee, "A group-theoretic framework for data augmentation," arXiv preprint arXiv:1907.10905, 2020.
- [24] A. Agostini and E. Celaya, "Exploiting domain symmetries in reinforcement learning with continuous state and action spaces," in *2009 International Conference on Machine Learning and Applications*. IEEE, 2009, pp. 331–336.
- [25] F. Abdolhosseini, H. Y. Ling, Z. Xie, X. B. Peng, and M. van de Panne, "On learning symmetric locomotion," in *Motion, Interaction and Games*, 2019, pp. 1–10.
- [26] Y. Lin, J. Huang, M. Zimmer, Y. Guan, J. Rojas, and P. Weng, "Invariant transform experience replay: Data augmentation for deep reinforcement learning," *IEEE Robotics and Automation Letters*, vol. 5, no. 4, pp. 6615–6622, 2020.
- [27] S. Mishra, A. Abdolmaleki, A. Guez, P. Trochim, and D. Precup, "Augmenting learning using symmetry in a biologically-inspired domain," arXiv preprint arXiv:1910.00528, 2019.
- [28] D. Silver, A. Huang, C. J. Maddison, A. Guez, L. Sifre, G. Van Den Driessche, J. Schrittwieser, I. Antonoglou, V. Panneershelvam, M. Lanctot *et al.*, "Mastering the game of go with deep neural networks and tree search," *nature*, vol. 529, no. 7587, pp. 484–489, 2016.
- [29] R. J. Griffin, G. Wiedebach, S. Bertrand, A. Leonessa, and J. Pratt, "Walking stabilization using step timing and location adjustment on the humanoid robot, atlas," in *2017 IEEE/RSJ International Conference on Intelligent Robots and Systems (IROS)*. IEEE, 2017, pp. 667–673.
- [30] H. Jeong, I. Lee, J. Oh, K. K. Lee, and J.-H. Oh, "A robust walking controller based on online optimization of ankle, hip, and stepping strategies," *IEEE Transactions on Robotics*, vol. 35, no. 6, pp. 1367–1386, 2019.
- [31] M. Khadiv, A. Herzog, S. A. A. Moosavian, and L. Righetti, "Walking control based on step timing adaptation," *IEEE Transactions on Robotics*, 2020.
- [32] S. Gu, E. Holly, T. Lillicrap, and S. Levine, "Deep reinforcement learning for robotic manipulation with asynchronous off-policy updates," in *2017 IEEE international conference on robotics and automation (ICRA)*. IEEE, 2017, pp. 3389–3396.
- [33] M. Abreu, N. Lau, A. Sousa, and L. P. Reis, "Learning low level skills from scratch for humanoid robot soccer using deep reinforcement learning," in *2019 IEEE International Conference on Autonomous Robot Systems and Competitions (ICARSC)*. IEEE, 2019, pp. 1–8.
- [34] A. J. Ratner, H. Ehrenberg, Z. Hussain, J. Dunnmon, and C. Ré, "Learning to compose domain-specific transformations for data augmentation," in *Advances in neural information processing systems*, 2017, pp. 3236–3246.
- [35] C. Yang, K. Yuan, W. Merkt, T. Komura, S. Vijayakumar, and Z. Li, "Learning whole-body motor skills for humanoids," in *2018 IEEE-RAS 18th International Conference on Humanoid Robots (Humanoids)*. IEEE, 2018, pp. 270–276.
- [36] V. Tsounis, M. Alge, J. Lee, F. Farshidian, and M. Hutter, "Deepgait: Planning and control of quadrupedal gaits using deep reinforcement learning," *IEEE Robotics and Automation Letters*, vol. 5, no. 2, pp. 3699–3706, 2020.
- [37] B. Ravindran and A. G. Barto, "Symmetries and model minimization in markov decision processes," USA, Tech. Rep., 2001.
- [38] R. S. Sutton and A. G. Barto, *Reinforcement learning: An introduction*. MIT press, 2018.
- [39] J. Schulman, P. Moritz, S. Levine, M. Jordan, and P. Abbeel, "High-dimensional continuous control using generalized advantage estimation," *CoRR*, vol. 1506.02438, 2018.
- [40] E. Coumans and Y. Bai, "Pybullet, a python module for physics simulation for games, robotics and machine learning," <http://pybullet.org>, 2016–2020.
- [41] R. Robinson, W. Herzog, and B. M. Nigg, "Use of force platform variables to quantify the effects of chiropractic manipulation on gait symmetry," *Journal of manipulative and physiological therapeutics*, vol. 10, no. 4, pp. 172–176, 1987.